

A framework for interpreting regularized state estimation

NOZOMI SUGIURA * AND SHUHEI MASUDA

Research Institute for Global Change, JAMSTEC, Yokosuka, Japan

YOSUKE FUJII AND MASAFUMI KAMACHI

Meteorological Research Institute, Tsukuba, Japan

YOICHI ISHIKAWA AND TOSHIYUKI AWAJI

Data Research Center for Marine-Earth Sciences, JAMSTEC, Yokohama, Japan

arXiv:1511.04790v1 [physics.data-an] 16 Nov 2015

* *Corresponding author address:* Nozomi Sugiura, Research Institute for Global Change, Japan Agency for Marine-Earth Science and Technology, 2-15 Natsushima-cho, Yokosuka 237-0061, Japan.

E-mail: nsugiura@jamstec.go.jp

ABSTRACT

Four-dimensional variational (4D-Var) data assimilation on a seasonal-to-interdecadal time-scale under the existence of unstable modes can be viewed as an optimization problem of synchronized, coupled chaotic systems. The problem is tackled by adjusting initial conditions to bring all stable modes closer to observations and by using a continuous guide to direct unstable modes toward a reference time series. This interpretation provides a consistent and effective procedure for solving problems of long-term state estimation. By applying this approach to an ocean general circulation model with a parameterized vertical diffusion procedure, it is demonstrated that tangent linear and adjoint models in this framework should have no unstable modes and hence be suitable for tracking persistent signals. This methodology is widely applicable to extend the assimilation period in 4D-Var.

1. Introduction

The 4-dimensional variational (hereafter, 4D-Var) data assimilation method has the advantage that it provides a model time-trajectory fit to observations and hence can create a dynamically self-consistent data set. In particular, it enables estimation of the long-term ocean state, which is desirable to better understand climate change in conjunction with seasonal-to-interdecadal variation (e.g., Stammer et al. 2002; Wunsch and Heimbach 2007; Köhl and Stammer 2008; Masuda et al. 2010).

The 4D-Var method solves a least-squares problem by using gradient information derived from tangent linear and adjoint integrations. The tangent linear operator is defined as the Jacobian matrix of a model's nonlinear propagation operator, and the adjoint operator is defined as its transpose. Despite the existence of these clear mathematical definitions, tangent linear and adjoint models (hereafter, linear models) that are algebraically approximate are often used in practical oceanic or atmospheric applications of 4D-Var data assimilation. These inexact linear models are favored not because of the difficulties in exact differentiation of a complex ocean general circulation model (OGCM), but because algebraically exact linear models sometimes generate undesirably strong sensitivities, which give rise to inappropriate gradient information for optimizations on a seasonal-to-interdecadal time scale (e.g., Lea et al. 2002; Hoteit et al. 2005; Köhl and Willebrand 2008). Apart from the possibility of numerical instabilities, which cannot be totally ruled out in some applications (e.g., Zhu and Kamachi 2000), these strong sensitivities have a dynamical origin associated with instabilities arising from rapidly growing perturbations that are not necessarily relevant to the phenomena of interest (Buizza 1994). Previous studies have used some modified lin-

ear models to address this difficulty and have achieved successful optimization (Hoteit et al. 2005; Sugiura et al. 2008; Mazloff et al. 2010), but the rationale for their use is still unclear. Thus, a systematic procedure for defining the optimization problem and estimating the long-term ocean state remains elusive.

It is well-known in nonlinear dynamical system research that a chaotic system can be stabilized by being coupled with an external system through the mechanism of chaos synchronization (Pecora and Carroll 1990; Pyragas 1993). Here “coupling” refers to a connection between two similar dynamical systems in phase space, not to a physical coupling of air and sea. A similar concept has long been utilized in linear control theory. The Luenberger observer (Luenberger 1964) is a modeled system that mimics the truth, and the time evolution of the observer is described by the sum of the time-stepping operator of the true system and a coupling term, which acts as an attractive force to the truth along some of the degrees of freedom possessed by the original state. If the error between the two systems goes to zero, the observer is synchronized with the truth, or follows exactly the same orbit as the truth. This condition is called the “observability condition,” and it also is characterized by negative conditional Lyapunov exponents for all modes existing in the observer system. So et al. (1994) extended this concept to nonlinear systems and established the necessary conditions for the coupling term in a nonlinear observer to achieve synchronization between the truth and the model. These conditions are that the variational equation for the observer should be Lyapunov-stable and that the image of the Jacobi matrix of the coupling term should remain in unstable subspace so as not to contaminate the stable modes of the original system. Later, Abarbanel et al. (2010) defined and solved a variational problem with a cost function that measures how well the synchronization is achieved between the truth and the

nonlinear observer.

In this paper, we examine these issues from the perspective of regularization, that is, the smoothing of the cost function surface of Abarbanel et al. (2010), by assuming synchronized coupled chaotic systems. We then discuss how to construct appropriate linear models for an ocean state estimation that uses an assimilation window longer than the characteristic period of the fastest growing mode. We also introduce some regularization procedures into the vertical diffusion scheme of a realistic OGCM for practical use.

2. Formulation

a. Problem setting

Data assimilation can be viewed as a problem of synchronizing two dynamical systems, one representing *truth* and the other representing a *model* (Yang et al. 2006). The former is often called the *master system*, whereas the latter is called the *slave system*, because the flow of information is unidirectional from the former to the latter (Duane et al. 2006).

For instance, Abarbanel et al. (2010) achieved a synchronization between two such systems by introducing a restoring term to the model equation that incorporates as many independent pieces of observational information, or *truth*, as there are distinct unstable directions in phase space along which instabilities occur in the synchronization manifold. (See Appendix A for details.) The most important implication of their approach is that to have a stable solution procedure for data assimilation, the model should provide some restoring terms, or coupling terms, toward a *truth* to suppress the instabilities that may occur in some

modes. In the case of ocean data assimilation, although the model that describes the ocean dynamical system exhibits an unstable nature, we usually cannot provide enough observations to assign to all of the unstable directions. We rather focus on chaos synchronization between the two systems, or the stabilization of the slave system by the continuous guidance of some master system. The concept of synchronization is still applicable even if *truth* is replaced by some other external system with an evolution law similar to that of the *model*. That is, although in geophysical applications we usually do not have enough observational information to restore all distinct unstable directions, we are still able to treat the information from *truth* as hidden variables and assign them tentative values, provided by a model integration from an updated guess of the initial condition (called a “reference time series” hereafter). Under the assumption that this kind of additional external information is available, a regularized data assimilation problem, of minimizing a cost function (Eq. (1)) subject to constraints (Eqs. (3) and (16)), is defined as follows.

The original 4D-Var problem in an incremental formulation (e.g., Courtier et al. 1994; Lawless et al. 2005; Trémolet 2007) is defined as the problem of finding an optimal initial condition, under the constraint of observations, that approximately minimizes the cost function

$$\begin{aligned} \mathcal{J}(\boldsymbol{\psi}; \boldsymbol{\theta}) = & \frac{1}{2} (\boldsymbol{\theta} + \boldsymbol{\psi} - \boldsymbol{\theta}_b)^T \mathbf{B}^{-1} (\boldsymbol{\theta} + \boldsymbol{\psi} - \boldsymbol{\theta}_b) \\ & + \frac{1}{2} \sum_{n=1}^N (\mathbf{H}(\mathbf{x}) - \mathbf{x}^{obs})^T \mathbf{R}^{-1} (\mathbf{H}(\mathbf{x}) - \mathbf{x}^{obs}) \Big|_{t=t_n}, \end{aligned} \quad (1)$$

subject to

$$\dot{\mathbf{x}} = \mathbf{f}(\mathbf{x}), \quad \mathbf{x}(0) = \boldsymbol{\theta} + \boldsymbol{\psi}, \quad (2)$$

with the reference time series for gradient calculation defined as

$$\dot{\mathbf{y}} = \mathbf{f}(\mathbf{y}), \quad \mathbf{y}(0) = \boldsymbol{\theta}, \quad (3)$$

where n is the time index, \mathbf{B} is the background error covariance matrix, \mathbf{R} is the observational error covariance matrix, $\boldsymbol{\theta}$ is the initial state of the reference system, $\boldsymbol{\psi}$ is the difference between the initial states of the estimated systems and the reference system, $\boldsymbol{\theta}_b$ is a firstguess for the initial state of the reference system, \mathbf{x} denotes the estimated time series integrated from the initial state $\boldsymbol{\theta} + \boldsymbol{\psi}$, \mathbf{y} denotes the reference time series integrated from the initial state $\boldsymbol{\theta}$, and \mathbf{x}^{obs} denotes the observations. The optimization problem will be approximately solved for the control variable $\boldsymbol{\psi}$, a procedure that is called the inner loop. Note that the inner loop only concerns the incremental state $\mathbf{v} = \mathbf{x} - \mathbf{y}$. Although $\boldsymbol{\theta}$, or \mathbf{y} , is usually updated as well using the information from the optimized value of $\boldsymbol{\psi}$, which is called the outer loop of incremental 4D-Var, we concentrate here on the optimization of $\boldsymbol{\psi}$, or \mathbf{v} , in the inner loop.

For simplicity, we assume in Eq. (1) that $\boldsymbol{\theta} = \boldsymbol{\theta}_b$, $\mathbf{B} = \sigma_b^2 \mathbf{I}$, $\mathbf{R} = \sigma_o^2 \mathbf{I}$, $\mathbf{H} = \mathcal{I}$, the identity operator, and all observations \mathbf{x}^{obs} are located at the end of the assimilation window ($t = t_N$). Accordingly, we can consider that the model operator \mathbf{M} assigns to every initial state $\mathbf{x}(0)$ a final state $\mathbf{x}(t_N)$. In this setting, the incremental 4D-Var cost function in quadratic form is written as

$$\mathcal{J}(\boldsymbol{\psi}) = \frac{1}{2\sigma_b^2} \boldsymbol{\psi}^T \boldsymbol{\psi} + \frac{1}{2\sigma_o^2} (\mathbf{M}\boldsymbol{\psi} - \mathbf{d})^T (\mathbf{M}\boldsymbol{\psi} - \mathbf{d}), \quad (4)$$

$$\mathbf{d} = \mathbf{x}^{obs} - \mathbf{M}(\boldsymbol{\theta}_b), \quad (5)$$

where \mathbf{M} is the derivative of the model operator \mathbf{M} with respect to the initial condition $\boldsymbol{\psi}$ of the incremental state \mathbf{v} . It is convenient to express \mathbf{M} in the form of a singular value

decomposition (Johnson et al. 2006):

$$\mathbf{M} = \sum_j \mathbf{U}_j \sigma_j \mathbf{V}_j^T, \quad (6)$$

$$\sigma_1 > \sigma_2 > \cdots > \sigma_{j_s-1} > 1 \geq \sigma_{j_s} > \cdots > \sigma_r \sim 0, \quad (7)$$

where r is the rank of \mathbf{M} , j_s indicates the first stable mode, and, for each mode j , \mathbf{V}_j is the right singular vector, \mathbf{U}_j is the left singular vector, and σ_j is the singular value, or the growth rate during the assimilation window. Each set of singular vectors is orthonormal and can be regarded as a finite-interval counterpart of the Lyapunov vectors (Legras and Vautard 1996). Using this decomposition, the gradient used for the inner loop optimization is expressed as

$$\nabla \mathcal{J} = \frac{1}{\sigma_b^2} \boldsymbol{\psi} + \frac{1}{\sigma_o^2} \mathbf{M}^T (\mathbf{M} \boldsymbol{\psi} - \mathbf{d}) \quad (8)$$

$$= \sigma_o^{-2} \sum_j [(\mu^2 + \sigma_j^2) (\mathbf{V}_j^T \boldsymbol{\psi}) - \sigma_j \mathbf{U}_j^T \mathbf{d}] \mathbf{V}_j, \quad (9)$$

where $\mu = \sigma_o/\sigma_b$. If the fastest growth rate σ_1 becomes many orders of magnitude larger than 1 due to the extension of the assimilation window beyond the predictability, then the cost function \mathcal{J} becomes so sensitive to the initial condition $\boldsymbol{\psi}$, or the magnitude of $\nabla \mathcal{J}$ becomes so large, that any gradient-based solution method can hardly solve the stationary problem $\nabla \mathcal{J} = 0$, or more precisely, almost infinite precision is required for an initial condition to solve it. This situation corresponds to what Abarbanel et al. (2010) called the irregularity of the cost function surface.

Even in that situation, we can still solve the problem in a reduced control space spanned by the stable singular vectors $\mathbf{V}_{j_s}, \mathbf{V}_{j_s+1}, \dots$. In fact, using a projection operator $\mathcal{P}_s =$

$\sum_{j \geq j_s} \mathbf{V}_j \mathbf{V}_j^T$, we can define a new cost function:

$$\begin{aligned} \tilde{\mathcal{J}}(\boldsymbol{\psi}) &\equiv \mathcal{J} \left(\sum_{j \geq j_s} \mathbf{V}_j \mathbf{V}_j^T \boldsymbol{\psi} \right) \\ &= \frac{1}{2\sigma_b^2} \sum_{j \geq j_s} (\mathbf{V}_j^T \boldsymbol{\psi})^2 + \frac{1}{2\sigma_o^2} \left(\tilde{\mathbf{M}} \boldsymbol{\psi} - \mathbf{d} \right)^T \left(\tilde{\mathbf{M}} \boldsymbol{\psi} - \mathbf{d} \right), \end{aligned} \quad (10)$$

$$\tilde{\mathbf{M}} = \sum_{j \geq j_s} \mathbf{U}_j \sigma_j \mathbf{V}_j^T, \quad (11)$$

of which the gradient

$$\nabla \tilde{\mathcal{J}} = \sigma_o^{-2} \sum_{j \geq j_s} [(\mu^2 + \sigma_j^2) (\mathbf{V}_j^T \boldsymbol{\psi}) - \sigma_j \mathbf{U}_j^T \mathbf{d}] \mathbf{V}_j \quad (12)$$

is now appropriately derived using the growth rates $\sigma_j \leq 1$ ($j \geq j_s$). The point is that the definition of the new cost function $\tilde{\mathcal{J}}$ is based on identifying the stable singular vectors. If the image of the projection operator \mathcal{P}_s contains even a very small fraction of unstable modes, then it will grow exponentially, and thus the reduced treatment will fail.

In practice, a complete set of stable singular vectors cannot be perfectly prescribed in an ocean data assimilation, and thus we should use instead a modified model $\hat{\mathbf{M}}$ which has a linearized dynamics $\hat{\mathbf{M}}$ similar to \mathbf{M} but exhibits a stable evolution. If each growth rate σ_j is assumed to be modified to $\hat{\sigma}_j \leq 1$ in the linearized dynamics $\hat{\mathbf{M}}$, then we can define another new cost function $\hat{\mathcal{J}}$ as

$$\hat{\mathcal{J}}(\boldsymbol{\psi}) = \frac{1}{2\sigma_b^2} \boldsymbol{\psi}^T \boldsymbol{\psi} + \frac{1}{2\sigma_o^2} \left(\hat{\mathbf{M}} \boldsymbol{\psi} - \mathbf{d} \right)^T \left(\hat{\mathbf{M}} \boldsymbol{\psi} - \mathbf{d} \right), \quad (13)$$

$$\hat{\mathbf{M}} = \sum_j \mathbf{U}_j \hat{\sigma}_j \mathbf{V}_j^T, \quad (14)$$

of which the gradient

$$\nabla \hat{\mathcal{J}} = \sigma_o^{-2} \sum_j [(\mu^2 + \hat{\sigma}_j^2) (\mathbf{V}_j^T \boldsymbol{\psi}) - \hat{\sigma}_j \mathbf{U}_j^T \mathbf{d}] \mathbf{V}_j \quad (15)$$

is also appropriately derived using the growth rates $\hat{\sigma}_j \leq 1$ ($j = 1, 2, \dots$). Note that this cost function $\hat{\mathcal{J}}$ includes $\tilde{\mathcal{J}}$ as a special case with $\hat{\sigma}_j = 0$ ($j < j_s$) and $\hat{\sigma}_j = \sigma_j$ ($j \geq j_s$), except for a slight difference in the background term. To prepare a model $\hat{\mathbf{M}}$ appropriate for $\hat{\mathcal{J}}$, we introduce into the nonlinear model a restoring term, similar to that of Abarbanel et al. (2010), that is intended to suppress the unstable modes that may arise at every moment of the integration of its linear models. In what follows, the mapping $\hat{\mathbf{M}} : \mathbf{x}(0) \mapsto \mathbf{x}(t_N)$ is represented in the form of a differential equation for \mathbf{x} (e.g., Eq. (16)).

Now we are ready to specify how regularized 4D-Var makes tractable optimization problems that are insoluble by the original 4D-Var. The modification of the constraints on the cost function (Eq. (1)) is made by assuming the following form of the model evolution instead of Eq. (2):

$$\dot{\mathbf{x}} = \mathbf{f}(\mathbf{x}) + \epsilon \mathbf{g}(\mathbf{x}, \mathbf{y}), \quad \mathbf{x}(0) = \boldsymbol{\theta} + \boldsymbol{\psi}, \quad (16)$$

where \mathbf{g} is an anti-symmetric function and ϵ is a coupling intensity. In this formulation, we have a master system \mathbf{y} described by a nonlinear model integrated from a known initial state $\boldsymbol{\theta}$, and a slave system \mathbf{x} described by a model, using the same equation but with a coupling term between them, that is integrated from an estimated initial state $\boldsymbol{\theta} + \boldsymbol{\psi}$. The slave system is attracted to the master system in phase space through the coupling term (Figure 1). As shown in Appendix B, the variational equation (the tangent linear equation that describes sensitivities) along the transverse direction $\mathbf{v} = \mathbf{x} - \mathbf{y}$ on the synchronization manifold $\mathbf{x} = \mathbf{y}$ is

$$\delta \dot{\mathbf{v}} = (\mathbf{D}\mathbf{f} + \epsilon \mathbf{D}_1 \mathbf{g}) \delta \mathbf{v}, \quad (17)$$

which is decoupled from the sensitivities of the master system.

The largest conditional Lyapunov exponent for the variational equation (17) can be reduced by properly defining the coupling function \mathbf{g} (e.g., Pyragas 1993). To that end, \mathbf{g} should be designed as an attractive force so that $\mathbf{D}_1\mathbf{g}$ provides a damping effect on the eigenspaces with positive Lyapunov exponents of $\mathbf{D}\mathbf{f}$, which correspond to unstable directions in phase space.

We can characterize the regularized 4D-Var method in comparison with the other methods mentioned as follows. The method of Abarbanel et al. (2010) adjusts initial conditions and restoring coefficients to bring all unstable but stabilized modes closer to observations and use a continuous guide to bring the model’s unstable modes toward observational data. The original 4D-Var method adjusts initial conditions to bring all modes closer to observations. The regularized 4D-Var method adjusts initial conditions to bring all stable modes closer to observations and uses a continuous guide to direct the unstable modes toward the reference time series. The similarity between this method and that of Abarbanel et al. (2010) lies in the use of regularization, which makes all modes stable in the model with some guidance by external systems (the reference time series and observations, respectively).

As is shown below, this framework offers a unified interpretation of the existing regularization methods with modified adjoint models (e.g., Hoteit et al. 2005). See Appendix C for a discrete-time version of the regularized 4D-Var problem and the details of the solution algorithm for practical use.

Here we show an application of this kind of regularization to linear models for data assimilation, where coupled master-slave systems are implicitly assumed. Horizontal eddy activities are a major cause of instability in the ocean, resulting in large sensitivities of linear models. Hoteit et al. (2005) suppressed these large sensitivities by introducing a horizon-

tal diffusion coefficient and a horizontal viscosity coefficient (horizontal mixing coefficients hereafter) larger than the ones in the forward model. In the context of regularization, we interpret their method as follows. The object to which data assimilation is applied is defined by substituting $\mathbf{f}(\mathbf{x}) = \mathbf{f}_0(\mathbf{x}) + \mathbf{K}\nabla^2\mathbf{x}$ and $\mathbf{g}(\mathbf{x}, \mathbf{y}) = -\mathbf{K}\nabla^2(\mathbf{y} - \mathbf{x})$ into Eqs. (3), (16), and (17). Because the coupling term is related to a term in the original nonlinear model operator \mathbf{f} , here we set the relevant term apart from the rest of the terms \mathbf{f}_0 . The nonlinear and variational equations for this case are

$$\dot{\mathbf{y}} = \mathbf{f}_0(\mathbf{y}) + \mathbf{K}\nabla^2\mathbf{y}, \quad (18)$$

$$\dot{\mathbf{x}} = \mathbf{f}_0(\mathbf{x}) + \mathbf{K}\nabla^2\mathbf{x} - \epsilon\mathbf{K}\nabla^2(\mathbf{y} - \mathbf{x}), \quad (19)$$

and

$$\delta\dot{\mathbf{v}} = [\mathbf{D}\mathbf{f}_0 + (1 + \epsilon)\mathbf{K}\nabla^2] \delta\mathbf{v}, \quad (20)$$

where \mathbf{f}_0 is the model operator excluding the mixing terms, $\mathbf{K} \geq 0$ represents the horizontal mixing coefficients (constant tensor), ∇^2 denotes the horizontal Laplacian, and ϵ is the coupling intensity.

Thus, the variational equation is the same as the original tangent linear equation except that the mixing tensor \mathbf{K} is enhanced to $(1 + \epsilon)\mathbf{K}$. That is, the enhanced horizontal mixing coefficients are explained by coupling with a master system.

b. Role of the coupling term

For the regularization to work properly, an efficient coupling function must meet three criteria:

- i. For the separation of the sensitivities, \mathbf{g} must be antisymmetric.
- ii. For the stability of the \mathbf{v} -system, the evolution governed by $\dot{\delta\mathbf{v}} = (\mathbf{D}\mathbf{f} + \epsilon\mathbf{D}_1\mathbf{g})\delta\mathbf{v}$ must have no positive Lyapunov exponents.
- iii. For the similarity between the sensitivities of the \mathbf{v} -system and \mathbf{y} -system, the image of $\mathbf{D}_1\mathbf{g}$ should lie mainly in an unstable subspace in order not to contaminate too much the evolution of Lyapunov vectors in the originally stable subspace. In other words, the stable subspace of the \mathbf{v} -system should not lose its original features in the stable subspace of the \mathbf{y} -system.

One of the ideal coupling functions that fully satisfies conditions i and iii is found in the master and slave systems of Abarbanel et al. (2010), given here as Eqs. (A3), (A4), and (A5) in Appendix A. The variational equation for the difference between the \mathbf{x} - and \mathbf{y} -systems is

$$\dot{\delta\mathbf{v}} = \left(\mathbf{D}\mathbf{f} - \begin{bmatrix} \mathbf{C}(t) & \\ & \mathbf{0}_{M-M_u} \end{bmatrix} \right) \delta\mathbf{v}. \quad (21)$$

Abarbanel et al. (2010) also controlled the function $\mathbf{C}(t)$ to meet condition ii by a variational method (Eq. (A1) in Appendix A). When it is difficult to separate the unstable directions cleanly, as they did, such as in the case of a high dimensional system, we should find an acceptable candidate for \mathbf{g} that reasonably satisfies the above conditions.

Below we discuss the role of the coupling term $\epsilon\mathbf{g}$ and how it should be efficiently defined in practical applications, taking the case of horizontal mixing coefficients as an example. We assume here, for simplicity, that $\delta\mathbf{v}$ corresponds to a function of 1-dimensional space s and

time t , $\delta v(s, t)$, which is expressed as a Fourier series on a finite spatial interval $[0, L]$,

$$\delta v(s, t) = \sum_{j=0}^{\infty} \delta v_j(s, t), \quad (22)$$

$$\delta v_j(s, t) \equiv a_j^0(t) \cos\left(\frac{2\pi j}{L}s\right) + a_j^1(t) \sin\left(\frac{2\pi j}{L}s\right). \quad (23)$$

The action of \mathbf{Df}_0 on the j -th mode is given by a growth rate λ_j ,

$$\mathbf{Df}_0 \delta v_j = \lambda_j \delta v_j. \quad (24)$$

Substituting the above expressions into Eq. (20), we get

$$\frac{\dot{a}_j^l}{a_j^l} = \lambda_j - (1 + \epsilon)K \left(\frac{2\pi j}{L}\right)^2, \quad l = 0, 1, \quad (25)$$

where the mixing coefficients are treated as a scalar constant K for simplicity. The action of the coupling term $\mathbf{D}_1 \mathbf{g}$ is represented here by the terms $-K(2\pi j/L)^2$, which constitute an attractive force to the master system along the high-wavenumber subspace in substitution for the unstable subspace; that is, the coupling term attracts the two states along high-wavenumber horizontal variability. The larger the wavenumber is, the more strongly \mathbf{x} is attracted to \mathbf{y} .

The solutions of Eq. (25) are

$$a_j^l(t) = a_j^l(0) \exp\left\{\left[\lambda_j - (1 + \epsilon)K \left(\frac{2\pi j}{L}\right)^2\right]t\right\}, \quad l = 0, 1. \quad (26)$$

If we have $\epsilon = 0$ ($\epsilon > 0$) in Eq. (26), then it describes the error growth of the j -th Fourier mode of the \mathbf{y} -system (the \mathbf{v} -system). The condition for stabilizing the \mathbf{v} -system (condition ii) is that for every j that satisfies $\lambda_j - K \left(\frac{2\pi j}{L}\right)^2 > 0$ the following must be satisfied:

$$\lambda_j - (1 + \epsilon)K \left(\frac{2\pi j}{L}\right)^2 \leq 0. \quad (27)$$

The application of $\epsilon > 0$ also has an influence on the originally stable modes which satisfy $\lambda_j - K \left(\frac{2\pi j}{L}\right)^2 < 0$. To minimize the impact of the coupling term on the stable subspace of the original system (condition iii), we should choose the smallest possible ϵ that satisfies the stability condition of Eq.(27). Note that we are not directly assigning a value to ϵ for any actual application, because we made here several assumptions about the system configuration and parameters.

In terms of the analysis field, the effect of the coupling term on the solution is assessed as follows. For the original 4D-Var problem, the minimizer of the cost function (Eq. (4)) is formally written with singular vectors as

$$\boldsymbol{\psi}_a = \sum_j \frac{\sigma_j^2}{\mu^2 + \sigma_j^2} \frac{\mathbf{U}_j^T \mathbf{d}}{\sigma_j} \mathbf{V}_j, \quad (28)$$

where $\mu = \sigma_o/\sigma_b$ (Johnson et al. 2006). Note that this solution is not available by any gradient method when the assimilation window is much longer than the predictability of the fastest mode. With the ideal coupling function (Eq. (21)), we now can write the minimizer of the regularized cost function (Eq. (13)) as

$$\hat{\boldsymbol{\psi}}_a = \sum_{j \geq j_s} \frac{\sigma_j^2}{\mu^2 + \sigma_j^2} \frac{\mathbf{U}_j^T \mathbf{d}}{\sigma_j} \mathbf{V}_j + \sum_{j < j_s} \frac{\hat{\sigma}_j^2}{\mu^2 + \hat{\sigma}_j^2} \frac{\mathbf{U}_j^T \mathbf{d}}{\hat{\sigma}_j} \mathbf{V}_j, \quad (29)$$

where $\hat{\sigma}_j$ ($j < j_s$) correspond to originally unstable modes that are stabilized by the additional coefficients $-\mathbf{C}(t)$ in Eq.(21). In this solution, all the modes in originally stable subspace ($j \geq j_s$) remain unchanged. Usually, these modes are also affected by the coupling term, and the solution is changed into

$$\hat{\boldsymbol{\psi}}_a = \sum_j \frac{\hat{\sigma}_j^2}{\mu^2 + \hat{\sigma}_j^2} \frac{\mathbf{U}_j^T \mathbf{d}}{\hat{\sigma}_j} \mathbf{V}_j, \quad (30)$$

where $\hat{\sigma}_j \leq 1$. The rate of deformation on the j -th mode of the analysis increment at time t_N , caused by the regularization, is estimated as

$$\frac{(\mathbf{U}_j, \hat{\mathbf{M}}\hat{\boldsymbol{\psi}}_a - \mathbf{M}\boldsymbol{\psi}_a)}{(\mathbf{U}_j, \mathbf{M}\boldsymbol{\psi}_a)} = \frac{\left(\frac{\hat{\sigma}_j}{\sigma_j}\right)^2 - 1}{1 + \left(\frac{\hat{\sigma}_j}{\mu}\right)^2}. \quad (31)$$

In the case of enhanced horizontal mixing (Eq. (26)), the rate of deformation is obtained by substituting

$$\frac{\hat{\sigma}_j}{\sigma_j} = \exp \left[-\epsilon K \left(\frac{2\pi j}{L} \right)^2 t_N \right]. \quad (32)$$

Given that $\hat{\sigma}_j$ should not be much larger than μ , Eqs. (31) and (32) represent the fact that the deformation in the analysis increment has a property of higher wave-number modes, possibly including stable modes, being damped more strongly.

Thus, the most significant effect of the coupling term is that it enables us to solve the optimization problem in an assimilation window much longer than the one used in the original 4D-Var method, although it confines the analysis increment to modes that are stable in the original dynamics, possibly causing some deformation in the increment. Nevertheless, an advantage of this approach is that we can extend the assimilation window with minimal additional computational cost other than that needed for the extended integration of the linear models.

3. Regularization for vertical mixing schemes

a. Methodology

In OGCMs, the oceanic instability associated with the vertical mixing process is expressed through the parameterization of mixed-layer dynamics. The sensitivity arising from the variation in this parameterization is a major obstacle to deriving effective gradient information in data assimilation. In some previous implementations (e.g., Hoteit et al. 2005; Gebbie et al. 2006; Köhl and Stammer 2008; Sugiura et al. 2008), this sensitivity was suppressed by not taking into account the variation of vertical diffusion coefficients or by omitting the linearization of the mixed-layer parameterization. Zhu et al. (2002) achieved a successful optimization by strategically ignoring the part of the variation of vertical diffusion coefficients that was caused by the variation of turbulent kinetic energy. Otherwise, the linear models of the ocean mixed-layer parameterization in these implementations would have caused the strong sensitivities to hide other important gradient information.

The passive treatment of the vertical diffusion coefficients in the 4D-Var method allows an interpretation that the model constraint is expressed by a slave system whose vertical diffusion coefficients are attracted to the ones defined in the master system. The model is constructed by substituting $\mathbf{f}(\mathbf{x}) = \mathbf{f}_0(\mathbf{x}) + \mathbf{k}(\mathbf{x}) \circ \nabla_z^2 \mathbf{x}$ and $\mathbf{g}(\mathbf{x}, \mathbf{y}) = (\mathbf{k}(\mathbf{y}) - \mathbf{k}(\mathbf{x})) \circ \nabla_z^2 (\mathbf{x} + \mathbf{y})/2$ into Eqs. (3), (16), and (17), where \circ denotes the entrywise product. The nonlinear and variational equations for the case with parameterized vertical diffusion coefficients are

then

$$\dot{\mathbf{y}} = \mathbf{f}_0(\mathbf{y}) + \mathbf{k}(\mathbf{y}) \circ \nabla_z^2 \mathbf{y}, \quad (33)$$

$$\dot{\mathbf{x}} = \mathbf{f}_0(\mathbf{x}) + \mathbf{k}(\mathbf{x}) \circ \nabla_z^2 \mathbf{x} + \epsilon (\mathbf{k}(\mathbf{y}) - \mathbf{k}(\mathbf{x})) \circ \nabla_z^2 \mathbf{u}, \quad (34)$$

$$\dot{\delta \mathbf{v}} = [\mathbf{Df}_0 + (1 - \epsilon)(\nabla_z^2 \mathbf{u}) \circ \mathbf{Dk} + \mathbf{k}(\mathbf{u}) \circ \nabla_z^2] \delta \mathbf{v}, \quad (35)$$

where \mathbf{f}_0 is the model operator, $\mathbf{k}(\mathbf{x}) \geq 0$ is the vertical diffusion coefficient (vector function of \mathbf{x}), $\mathbf{u} \equiv (\mathbf{x} + \mathbf{y})/2$, ∇_z^2 is the vertical Laplacian, and ϵ is the coupling intensity.

Eq. (35) means that the variational equation is the same as the original tangent linear equation except that the functional dependency of the diffusion coefficient \mathbf{k} is reduced to $(1 - \epsilon)\mathbf{Dk}$. The operation $(\nabla_z^2 \mathbf{u}) \circ \mathbf{Dk}$ has eigenvalues with indefinite sign, whereas the operation $\mathbf{k} \circ \nabla_z^2$ has only negative eigenvalues, the reduction of the former term can make the combined eigenstructure more stable. In particular, $\epsilon = 1$ means that the diffusion coefficient is completely prescribed, as was done by Sugiura et al. (2008), and smaller values correspond to a partially prescribed treatment.

Here we explain how regularization for vertical mixing schemes works by assuming a simplified situation. We assume that $\delta \mathbf{v}$ corresponds to a function of space s and time t , $\delta v(s, t)$. The space s does not necessarily mean a vertical 1-dimensional one, but it can also have horizontal spans. Introducing a space-time white noise η , which mimics the operation $(\nabla_z^2 \mathbf{u}) \circ \mathbf{Dk}$, we can describe the evolution of a mode in the \mathbf{v} -system (Eq. (35)) as

$$\dot{\delta v} = [\lambda + (1 - \epsilon)\eta + k\nabla^2] \delta v, \quad (36)$$

where δv is the function that represents the mode, λ is the growth rate caused by \mathbf{Df}_0 , and the background values of the mixing coefficients are represented by a scalar constant

k for simplicity. This noisy heat equation can exhibit complicated behavior due to the combination of a multiplicative noise term $\eta\delta v$ and a spatial correlation term $k\nabla^2\delta v$. By applying a logarithmic transformation $w = \log |\delta v|$, we get

$$\dot{w} = \lambda + (1 - \epsilon)\eta + k\nabla^2 w + k(\nabla w)^2, \quad (37)$$

which is known as the Kardar-Parisi-Zhang (KPZ) equation (Kardar et al. 1986). At least in the spatially 1-dimensional case, it is known that the nonlinear term $k(\nabla w)^2$ starts to become relevant when the magnitude of the noise $(1 - \epsilon)\eta$ exceeds a critical value (Kapral et al. 1994). Although much is unknown about the behavior in multi-dimensional cases, it is reported that the KPZ equation also captures the dynamics of the logarithmic error growth of a global weather model (Primo et al. 2007). If we assume the existence of a critical value, we can control the stability of the system by adjusting the noise level, which changes according to the value of ϵ . Apparently, $\epsilon = 1$ corresponds to a noiseless and stable situation, but if ϵ is less than a certain value the system can become unstable because of the roughness term $(\nabla w)^2$.

This kind of regularization, regarding coefficients with indefinite signs in a variational equation, might also be applicable to advection terms in an OGCM. We describe a possible procedure in Appendix D.

b. Case study

To demonstrate the effect of regularization on the sensitivities used in 4D-Var data assimilation into a state-of-the-art OGCM, we conducted a comparative study of three linearized treatments of the vertical diffusion coefficient in the master-slave setting described above.

The model we used was based on the Meteorological Research Institute (MRI) Community Ocean Model (Tsujino et al. 2010, 2011) developed by the Japan Meteorological Agency. It is a global model with a horizontal resolution of 1° longitude and 0.5° latitude with 51 vertical levels. The model is integrated under a climatological atmospheric forcing through a bulk parameterization scheme and with the mixed-layer closure scheme of Noh and Kim (1999). The model has an algorithmic structure in which the prognostic variables \mathbf{y} are integrated using the vertical diffusion coefficients \mathbf{k} , which are derived from the turbulent kinetic energy described by the prognostic mixed-layer dynamics for \mathbf{y} . Hence, the whole system with regularization is compactly described by Eqs. (33), (34), and (35). By using a tangent linear system governed by Eq. (35), we compared the effect of regularization under the following three settings.

- Case 1. The variation of the vertical diffusion coefficients is derived dynamically from the linearized version of the prognostic mixed-layer dynamics ($\epsilon = 0$ in Eqs. (34) and (35)).
- Case 2. The values of the vertical diffusion coefficients are prescribed by a master system ($\epsilon = 1$ in Eqs. (34) and (35)), as has been commonly done in previous studies (e.g., Sugiura et al. 2008).
- Case 3. The vertical diffusion coefficients are partly prescribed, but their variation, which is derived from the linearized version of the prognostic mixed-layer dynamics, is also partly taken into account ($\epsilon = 0.75$ in Eqs. (34) and (35)).

c. Results

We tested the stability of the linear models by evaluating the first backward Lyapunov vectors (Legras and Vautard 1996), that is, the modes that have grown the fastest, and the corresponding Lyapunov exponents. The j -th Lyapunov exponent is defined as

$$\lambda_j = \lim_{t \rightarrow \infty} \frac{1}{t} \log \|\boldsymbol{\xi}_j(t)\|, \quad (38)$$

by using $\boldsymbol{\xi}_j(t)$, the j -th Lyapunov vector at time t , and the norm of the vector,

$$\|\boldsymbol{\xi}_j(t)\|^2 = \frac{\sum_m (\xi_j^m(t))^2 \delta V_m}{\sum_m \delta V_m}, \quad (39)$$

where $\xi_j^m(t)$ is the m -th component of the j -th Lyapunov vector and δV_m is the volume element for the m -th component. The normalized quantity or vector for the j -th Lyapunov vector at time t is defined as

$$\hat{\boldsymbol{\xi}}_j = \frac{\boldsymbol{\xi}_j(t)}{\|\boldsymbol{\xi}_j(t)\|}. \quad (40)$$

Note that the first Lyapunov vector and the first Lyapunov exponent, which we calculate here, do not depend on the definition of the norm. If t is large, we can rewrite the j -th Lyapunov vector as

$$\boldsymbol{\xi}_j(t) = \hat{\boldsymbol{\xi}}_j(t) \|\boldsymbol{\xi}_j(t)\| \rightarrow \hat{\boldsymbol{\xi}}_j(t) e^{\lambda_j t}. \quad (41)$$

Care should be taken in the numerical computation of the Lyapunov vectors to avoid digit overflow due to their exponential growth. Thus, these were calculated from the results of an integration of the tangent linear model with periodic normalizations starting from an arbitrary initial perturbation (Benettin et al. 1980).

Taking into account the highly localized feature of Lyapunov vectors (Pazó et al. 2008), it is convenient to characterize the Lyapunov vector by the logarithmic quantity $\log |\hat{\xi}_j(t)|$, where $|\cdot|$ denotes the componentwise absolute value, and by the corresponding Lyapunov exponent λ_j . In this case study, the spatial pattern of $\log |\hat{\xi}_j(t)|$ is well represented by the one for sea surface temperature (SST) or for subsurface water temperature. Figure 2 shows the first backward Lyapunov vector for case 1, whose values are shown as the normalized quantities of $\log (|\delta\text{SST}|)$ (i.e., the logarithmic change in SST). The time change of the vector norm shows apparent growth corresponding to the Lyapunov exponent of 1.51 day^{-1} at a location near the oceanic tropical instability waves, suggesting the influence of sensitivity from the mixed-layer dynamics (Philander et al. 1986). Sensitivity at this short time scale is hardly applicable to state estimation using an assimilation window with a seasonal-to-interdecadal time scale.

Figure 3 shows the first backward Lyapunov vector for case 2, whose values are shown as the normalized quantities for $\log (|\delta T(z = 100 \text{ m})|)$ (i.e., the logarithmic temperature change at the 100-m isobath). The corresponding Lyapunov exponent is -0.001 day^{-1} , which means that temporal evolution during linear model integration is stable and that this method is relevant to seasonal-to-interdecadal scale climate research. The most persistent signal at the 100-m isobath appears in the area of the Antarctic Circumpolar Current, and the rapidly growing signals seen in case 1 disappear under the prescribed vertical diffusion coefficient of case 2. Note that the short-wavelength spatial structure in the approximate Lyapunov vector arises partly from the randomness of the initial perturbation because of the relatively short integration period (one year) of the tangent linear model.

Figure 4 shows the first backward Lyapunov vector for case 3, whose values are also shown

as the normalized quantities for $\log(|\delta T(z = 100 \text{ m})|)$, with the corresponding Lyapunov exponent of -0.001 day^{-1} . The vector exhibits almost the same structure and growth rate as case 2. The rapidly growing signals in case 1 also disappear under the partially prescribed vertical diffusion coefficients of case 3. The slight difference between cases 2 and 3 is probably caused mainly by the numerical truncation procedure, and the two procedures have basically identical results.

This comparison demonstrates that prescription of the vertical diffusion coefficient by a master equation, either totally ($\epsilon = 1$) or partially ($\epsilon = 0.75$), improves the stability of the slave system (Eq. (34)). Because the coupling term between the master and slave systems determines the extent to which the vertical diffusion coefficients in the OGCM system are prescribed, our result helps constraining the coupling strength necessary for regularization to function properly. Regularization settings that satisfy the condition $0.75 \leq \epsilon \leq 1$ should at least exhibit linearly stable behavior, and they will therefore be applicable to derive sensitivities in estimating long-term ocean states.

The result that stability is attained within some range of ϵ is consistent with our qualitative picture of how the regularization works, although the quantitative argument on the space-time error growth in conjunction with the KPZ equation still remains an issue for the future. At least it supports the interpretation that the regularization for vertical mixing schemes can be explained in the framework of synchronizing master and slave systems.

4. Discussion and conclusion

We have clarified the underlying structure behind the simplification of tangent linear and adjoint models commonly used in 4D-Var data assimilation in conjunction with a long assimilation window of seasonal-to-interdecadal time scale. The concept of coupled master-slave systems (e.g., Pyragas 1993) provides a unified interpretation of regularization techniques without introducing any ad-hoc linear models beyond adding a coupling term to the original equation. This framework enables us to focus on stable temporal developments in linear models, which are an essential component of 4D-Var data assimilation in climate research. The increase in stability helps us extracting slowly varying perturbations relevant to climate variations out of the many possible fundamental solutions of the linearized equation. We demonstrated the effect of this procedure numerically with an OGCM by changing the linearization of the functional dependency of the vertical diffusion coefficient. The stability of the system (Eq. (34)) is improved when the coefficient is partially or totally driven by a master system.

The 4D-Var optimization problem-setting and solution procedures for a practical application using this type of master-slave setting are formulated as the regularized 4D-Var method. Regularized 4D-Var in the seasonal-to-interdecadal time scale can be viewed as an inverse problem of finding the optimal initial condition for the synchronized manifold of a master-slave system subject to observational constraints. As the methodology is based on the stability of the synchronization manifold under the condition that the slave system is selectively attracted to the master system along unstable directions, the design of the coupling term between the two systems is crucial for setting up the problem for estimation

of the long-term ocean state. Our investigation of the existing applications of the coupling strategy has found that antisymmetric coupling functions that selectively damp the growth of unstable modes, by enhancing horizontal mixing in linear models or by suppressing sensitivities of vertical mixing schemes, are able to stabilize the slave system, but they may deform the stable modes at the same time. However, the contamination of the stable subspace can be reduced, at least in the case of enhanced horizontal mixing, by adjusting the coupling strength. A similar interpretation is applicable to the case of a multi-incremental setting (Courtier et al. 1994; Trémolet 2007) (for details, see Appendix E).

The master-slave methodology is a widely applicable regularization for climate research and long-term prediction activities, among many other effective regularization techniques such as the introduction of restoring terms with direct observational constraint (Abarbanel et al. 2010), the use of a time-distributed background error (Cullen 2010), and the use of reduced space spanned by leading vectors derived from empirical orthogonal function analysis (Hoteit and Köhl 2006; Yaremchuk et al. 2009).

As mentioned in Evensen (1997), weak constraint 4D-Var also enables us to extend the assimilation window longer than the predictability by adding a model error term to the model equation as an additive noise. It is implemented in practice by dividing an assimilation window into many short predictable sub-windows (Trémolet 2006), and thus it usually requires a more complicated system and more computational resources than strong constraint 4D-Var does. By treating the coupling intensity as an object to be minimized, the coupling term between master and slave systems can be regarded as a kind of model error in a weak constraint 4D-Var, but it should be in the form of a multiplicative noise (Hansen and Penland 2007) because it is dependent on the model state of the moment.

A weak constraint 4D-Var including additive and multiplicative noises may offer a more general framework for climate-scale data assimilation. Meanwhile, there still are many issues to be solved regarding its formulation, implementation, and computational efficiency in conjunction with regularization.

Acknowledgments.

We gratefully acknowledge many helpful comments and suggestions from several anonymous reviewers. This study was supported in part by the Japan Society for Promotion of Science [KAKENHI, Grant-in-aid for Young Scientists (B) 11024975] and the Ministry of Education, Culture, Sports, Science and Technology (MEXT), Japan [Research Program on Climate Change Adaptation (RECCA) 10101028]. The numerical calculations were carried out on the Earth Simulator of the Japan Agency for Marine-Earth Science and Technology (JAMSTEC).

APPENDIX A

The regularization of Abarbanel et al. (2010)

The data assimilation problem solved by Abarbanel et al. (2010) can be written as follows.

minimize

$$\mathcal{J}(\mathbf{x}(t_{1:N}), \mathbf{C}(t_{1:N})) = \frac{1}{2} \sum_{n=1}^N (\text{tr}(\mathbf{C}(t)^T \mathbf{C}(t)) + (\mathbf{x} - \mathbf{y})^T \mathbf{R}^{-1} (\mathbf{x} - \mathbf{y})) \Big|_{t=t_n}, \quad (\text{A1})$$

$$\mathbf{R}^{-1} \equiv \begin{bmatrix} \mathbf{I}_{M_u} & \\ & \mathbf{O}_{M-M_u} \end{bmatrix}, \quad (\text{A2})$$

subject to

$$\dot{\mathbf{y}} = \mathbf{f}(\mathbf{y}), \quad (\text{A3})$$

$$\dot{\mathbf{x}} = \mathbf{f}(\mathbf{x}) + \mathbf{g}(\mathbf{x}, \mathbf{y}), \quad (\text{A4})$$

$$\mathbf{g}(\mathbf{x}, \mathbf{y}) \equiv (\mathbf{D}_1 \mathbf{g})(\mathbf{x} - \mathbf{y}) = - \begin{bmatrix} \mathbf{C}(t) \\ \mathbf{O}_{M-M_u} \end{bmatrix} (\mathbf{x} - \mathbf{y}), \quad (\text{A5})$$

where \mathbf{y} is the state vector of the master system, \mathbf{x} is the state vector of the slave system, $\dot{\mathbf{x}}$ denotes the time derivative of \mathbf{x} , $\mathbf{D}_1 \mathbf{g}$ is the partial derivative of \mathbf{g} with respect to the first variable, $\mathbf{C}(t) \geq 0$, $\dim(\mathbf{x}) = M \times 1$, $\dim(\mathbf{y}) = M \times 1$, $\dim(\mathbf{C}) = M_u \times M_u$, M is the dimensions of the state space, and M_u is the dimensions of the unstable subspace spanned by the unit vectors $\{\mathbf{e}_i\}_{i=1,2,\dots,M_u}$. Obviously, the linear coupling function \mathbf{g} is antisymmetric $\mathbf{g}(\mathbf{y}, \mathbf{x}) = -\mathbf{g}(\mathbf{x}, \mathbf{y})$, and the image of $\mathbf{D}_1 \mathbf{g}$ always lies in the unstable subspace. With an

appropriate choice of \mathbf{C} , the time evolution of the model described by Eq. (A4) is stabilized by the constraint of observation \mathbf{y} . In other words, the variational equation,

$$\dot{\delta \mathbf{x}} = (\mathbf{Df} + \mathbf{D}_1 \mathbf{g}) \delta \mathbf{x}, \quad (\text{A6})$$

$$\mathbf{Df} \equiv \begin{bmatrix} \frac{\partial f_1}{\partial x_1} & \frac{\partial f_1}{\partial x_2} & \dots & \frac{\partial f_1}{\partial x_M} \\ \vdots & \vdots & & \vdots \\ \frac{\partial f_M}{\partial x_1} & \frac{\partial f_M}{\partial x_2} & \dots & \frac{\partial f_M}{\partial x_M} \end{bmatrix} \quad (\text{A7})$$

exhibits all non-negative Lyapunov exponents and realizes the synchronization of systems \mathbf{x} and \mathbf{y} , which makes the constraint by the coupling term less and less important as the state evolves, that is, $\mathbf{C}(t) \rightarrow 0$ as $t \rightarrow \infty$. This is the situation in which Abarbanel et al. (2010) considered the observational data to be properly assimilated into the model. The cost function of Eq. (A1) is composed of an observational error term and a penalty term indicating the restoring strength. When the synchronization $\mathbf{x} = \mathbf{y}$ is achieved after some transitional period, the cost converges to zero under ideal conditions. Abarbanel et al. (2010) solved the problem numerically by a “direct method” provided in the SNOPT software package (e.g., Barclay et al. 1998).

APPENDIX B

Decoupling the sensitivities

To Eqs. (3) and (16), we apply a change of variables from (\mathbf{x}, \mathbf{y}) to $(\mathbf{v}, \mathbf{y}') = (\mathbf{x} - \mathbf{y}, \mathbf{y})$.

Substituting $(\mathbf{x}, \mathbf{y}) = (\mathbf{y}' + \mathbf{v}, \mathbf{y}')$, we get

$$\dot{\mathbf{y}}' = \mathbf{f}(\mathbf{y}'), \quad (\text{B1})$$

$$\dot{\mathbf{y}}' + \dot{\mathbf{v}} = \mathbf{f}(\mathbf{y}' + \mathbf{v}) + \epsilon \mathbf{g}(\mathbf{y}' + \mathbf{v}, \mathbf{y}'). \quad (\text{B2})$$

The difference between these two equations is

$$\dot{\mathbf{v}} = \mathbf{f}(\mathbf{y}' + \mathbf{v}) - \mathbf{f}(\mathbf{y}') + \epsilon \mathbf{g}(\mathbf{y}' + \mathbf{v}, \mathbf{y}'). \quad (\text{B3})$$

Taking the first-order derivative of this equation, we get

$$\delta \dot{\mathbf{v}} = \mathbf{Df} \delta \mathbf{v} + \epsilon \mathbf{D}_1 \mathbf{g} (\delta \mathbf{y}' + \delta \mathbf{v}) + \epsilon \mathbf{D}_2 \mathbf{g} \delta \mathbf{y}', \quad (\text{B4})$$

where \mathbf{Df} is the derivative of \mathbf{f} and $\mathbf{D}_i \mathbf{g}$ is the partial derivative of \mathbf{g} with respect to the i -th variable.

If we assume the state vector to be in the neighborhood of the synchronization manifold $\mathbf{v} = 0$ or $\mathbf{x} = \mathbf{y}$, we can consider \mathbf{Df} , $\mathbf{D}_1 \mathbf{g}$, and $\mathbf{D}_2 \mathbf{g}$ to be defined on $(\mathbf{y}', \mathbf{y}')$ in the combined coordinate system for the master and slave systems, or we could also say on $(\mathbf{y}' + \mathbf{v}/2, \mathbf{y}' + \mathbf{v}/2) = ((\mathbf{x} + \mathbf{y})/2, (\mathbf{x} + \mathbf{y})/2)$. In that situation, $\mathbf{D}_1 \mathbf{g} = -\mathbf{D}_2 \mathbf{g}$ is deduced from the antisymmetry of \mathbf{g} .

APPENDIX C

Solving 4D-Var problems with regularization

We specify here a data assimilation setting with Eqs. (1), (3), and (16) in a tractable time-discretized form, and then discuss the details of the solution procedure. A complete nonlinear 4D-Var system with a master-slave setting aims to find the model state $(\boldsymbol{\psi}, \boldsymbol{\theta})$ at the initial time that approximately minimizes the cost function

$$\mathcal{J}(\boldsymbol{\psi}, \boldsymbol{\theta}) = \frac{1}{2} \|\boldsymbol{\theta} + \boldsymbol{\psi} - \boldsymbol{\theta}_b\|_{\mathbf{B}^{-1}}^2 + \frac{1}{2} \sum_{n=1}^N \|\mathbf{H}(\mathbf{x}_n) - \mathbf{x}_n^{obs}\|_{\mathbf{R}_n^{-1}}^2, \quad (\text{C1})$$

$$\mathbf{y}_n = \mathbf{F}(\mathbf{y}_{n-1}), \quad \mathbf{y}_0 = \boldsymbol{\theta}, \quad (\text{C2})$$

$$\mathbf{x}_n = \mathbf{F}(\mathbf{x}_{n-1}) - \epsilon \mathbf{G}(\mathbf{F}(\mathbf{x}_{n-1}), \mathbf{F}(\mathbf{y}_{n-1})), \quad \mathbf{x}_0 = \boldsymbol{\theta} + \boldsymbol{\psi}, \quad (\text{C3})$$

$$\begin{aligned} \nabla_{\boldsymbol{\psi}} \mathcal{J} &= \mathbf{B}^{-1} (\boldsymbol{\psi} + \boldsymbol{\theta} - \boldsymbol{\theta}_b) \\ &+ \sum_{n=1}^N \left(\frac{\partial \mathbf{x}_n}{\partial \boldsymbol{\psi}} \right)^T \mathbf{H}_n^T \mathbf{R}_n^{-1} \left[\mathbf{H}_n \left(\frac{\partial \mathbf{x}_n}{\partial \boldsymbol{\psi}} \right) \boldsymbol{\psi} + \mathbf{H}(\mathbf{x}_n(\boldsymbol{\theta})) - \mathbf{x}_n^{obs} \right] \end{aligned} \quad (\text{C4})$$

where n is the time index, \mathbf{B} is the background error covariance matrix, \mathbf{R} is the observational error covariance matrix, $\boldsymbol{\theta}$ is the initial state of the master system, $\boldsymbol{\psi}$ is the difference between the initial states of the master and slave systems, $\boldsymbol{\theta}_b$ is a first guess for the initial state of the master system, \mathbf{H} is an observation operator, \mathbf{x}_n^{obs} is an observation at time n , \mathbf{F} is the time-stepping operator for the original system, and \mathbf{G} is the coupling operator that satisfies $\mathbf{G}(\mathbf{y}, \mathbf{x}) = -\mathbf{G}(\mathbf{x}, \mathbf{y})$. Eq. (C4) shows the gradient of the cost function with respect to $\boldsymbol{\psi}$ that contains the tangent linear model $(\partial \mathbf{x}_n / \partial \boldsymbol{\psi})$ and the adjoint model $(\partial \mathbf{x}_n / \partial \boldsymbol{\psi})^T$.

Regarding the solution procedure for $\min_{\boldsymbol{\theta}} \left(\min_{\boldsymbol{\psi}} \mathcal{J} \right)$, we can solve the inner part (within the parentheses) by using a least-squares problem for $\boldsymbol{\psi}$ given $\boldsymbol{\theta}$, because the problem is regularized on the synchronization manifold, as presented in the main text. A possible strategy for the outer part is to update a guess for $\boldsymbol{\theta}$ to a new guess by a successive substitution method, $\boldsymbol{\theta}^{new} = \boldsymbol{\theta} + \operatorname{argmin}_{\boldsymbol{\psi}} \mathcal{J}(\boldsymbol{\psi}, \boldsymbol{\theta}) \equiv \mathbf{h}(\boldsymbol{\theta})$, which aims to find a fixed point $\boldsymbol{\theta}_* = \mathbf{h}(\boldsymbol{\theta}_*)$. This procedure restricts the analysis update direction to the difference between the master and slave systems. Although the convergence of $\boldsymbol{\theta}$ in the reduced space is not guaranteed in the strict sense as used in Gratton et al. (2008), if we can assume that the long-term evolution of the state \mathbf{x} is not affected much by the coupling correspondent \mathbf{y} , then the cost function satisfies the condition

$$\mathcal{J} \left(\operatorname{argmin}_{\boldsymbol{\psi}} \mathcal{J}(\boldsymbol{\psi}, \boldsymbol{\theta}), \boldsymbol{\theta} \right) \simeq \mathcal{J} \left(\mathbf{0}, \boldsymbol{\theta} + \operatorname{argmin}_{\boldsymbol{\psi}} \mathcal{J}(\boldsymbol{\psi}, \boldsymbol{\theta}) \right). \quad (\text{C5})$$

Note that the slave models used in these cost functions share a common initial state $\mathbf{x}_0 = \boldsymbol{\theta} + \operatorname{argmin}_{\boldsymbol{\psi}} \mathcal{J}(\boldsymbol{\psi}, \boldsymbol{\theta})$.

On the basis of the above assumption, the problem is approximately solved by the following iterative method, which is a variant of the Gauss-Newton algorithm (e.g., Lawless et al. 2005).

- i. Define a first guess field $\boldsymbol{\theta}^{(k)}$ at time t_0 and iteration number k . For the first iteration, $k = 0$, we choose $\boldsymbol{\theta}^{(0)} = \boldsymbol{\theta}_b$, the background state.
- ii. Find the linear least-square solution $\delta\boldsymbol{\psi} = \boldsymbol{\psi}^{(k)}$ of the incremental cost function

$$\begin{aligned} \hat{\mathcal{J}}(\delta\boldsymbol{\psi}, \boldsymbol{\theta}^{(k)}) &= \frac{1}{2} \left\| \boldsymbol{\theta}^{(k)} - \boldsymbol{\theta}_b + \delta\boldsymbol{\psi} \right\|_{\mathbf{B}^{-1}}^2 \\ &+ \frac{1}{2} \sum_{n=1}^N \left\| \mathbf{H} \left(\mathbf{x}_n(\mathbf{x}_0 = \boldsymbol{\theta}^{(k)}) \right) - \mathbf{x}_n^{obs} + \mathbf{H}_n \prod_{j=1}^n \{ (\mathbf{I} - \epsilon \mathbf{D}_1 \mathbf{G}_j) \mathbf{D} \mathbf{F}_j \} \delta\boldsymbol{\psi} \right\|_{\mathbf{R}_n^{-1}}^2 \end{aligned} \quad (\text{C6})$$

where \mathbf{DF} is the derivative of \mathbf{F} and $\mathbf{D}_1\mathbf{G}$ is the partial derivative of \mathbf{G} with respect to the first variable.

iii. Update the guess field using

$$\boldsymbol{\theta}^{(k+1)} = \boldsymbol{\theta}^{(k)} + \boldsymbol{\psi}^{(k)}. \quad (\text{C7})$$

iv. Repeat the procedure until a given convergence criterion is satisfied or a certain number of iterations has been performed. The analysis field at the initial time is then given by $(\boldsymbol{\psi}^a, \boldsymbol{\theta}^a) = (\boldsymbol{\psi}^{(K)}, \boldsymbol{\theta}^{(K)})$, where K is the total number of iterations performed.

Each iteration of this set of steps forms an outer loop. Within each outer loop, the minimization problem of step ii must be solved using an iterative procedure known as the inner loop. The outer loop should work because Eqs. (C5) and (C7) imply the following sequence of cost values:

$$\mathcal{J}(\boldsymbol{\psi}^{(k)}, \boldsymbol{\theta}^{(k)}) \simeq \mathcal{J}(\mathbf{0}, \boldsymbol{\theta}^{(k+1)}) > \mathcal{J}(\boldsymbol{\psi}^{(k+1)}, \boldsymbol{\theta}^{(k+1)}) \simeq \dots, \quad (\text{C8})$$

which is expected to decrease as the iteration proceeds.

Note that in previous applications (e.g., Hoteit et al. 2005; Sugiura et al. 2008), the number of inner loops in this procedure has been commonly set to 1, which is convenient because the state vector of the slave system is identical to that of the master system in the first iteration.

APPENDIX D

Regularization of advection terms

Suppose we have a pair of systems,

$$\dot{\mathbf{y}} = \mathbf{f}_0(\mathbf{y}) + \mathbf{y} \cdot \nabla \mathbf{y}, \quad (\text{D1})$$

$$\dot{\mathbf{x}} = \mathbf{f}_0(\mathbf{x}) + \mathbf{x} \cdot \nabla \mathbf{x} + \epsilon(\mathbf{y} - \mathbf{x}) \cdot \nabla \mathbf{u}, \quad (\text{D2})$$

where $\mathbf{u} = (\mathbf{x} + \mathbf{y})/2$, and the term $\mathbf{y} \cdot \nabla \mathbf{y}$ represents the two kinds of advection terms in an OGCM, $\boldsymbol{\mu} \cdot \nabla \boldsymbol{\tau}$ in a tracer equation and $\boldsymbol{\mu} \cdot \nabla \boldsymbol{\mu}$ in a momentum equation, where $\boldsymbol{\mu}$ is velocity and $\boldsymbol{\tau}$ is water temperature or salinity. The variational equation with respect to $\mathbf{v} = \mathbf{x} - \mathbf{y}$ in the neighborhood of $\mathbf{x} = \mathbf{y}$ is

$$\delta \dot{\mathbf{v}} = (\mathbf{D}\mathbf{f}_0 + \mathbf{u} \cdot \nabla) \delta \mathbf{v} + (1 - \epsilon) \delta \mathbf{v} \cdot \nabla \mathbf{u}. \quad (\text{D3})$$

If we reduce the contribution from the last term on the right-hand side of Eq. (D3) by setting $0 < \epsilon \leq 1$, the stability of the slave system possibly improves by a mechanism analogous to the stabilization by the treatment to the vertical mixing. In the particular case of $\epsilon = 1$, the system should become stable just as a linear advection-diffusion equation should because the terms related to the spatial gradient of the forward field are ignored, although this extreme setting might also cause significant loss of information about the sensitivities. There remain several implementational issues to be resolved before this method can be applied to an OGCM, for example, modifications to a conservative formulation or an effective discretization

into linearized OGCM codes. It is worth noting that the temporal averaging technique of the forward field for adjoint integration (Sugiura et al. 2008) could be viewed as a simplified variant of this treatment in the sense that the temporal averaging is expected to smooth the spatial gradient of the forward field used in linear models.

APPENDIX E

Interpretation for a multi-incremental setting

Substituting $\mathbf{g}(\mathbf{x}, \mathbf{y}) = (\mathcal{I} - \mathcal{P})(\mathbf{f}(\mathbf{y}) - \mathbf{f}(\mathbf{x}))$ into Eqs. (3), (16), and (17) yields nonlinear and variational equations for a multi-incremental setting,

$$\dot{\mathbf{y}} = \mathbf{f}(\mathbf{y}), \tag{E1}$$

$$\dot{\mathbf{x}} = \mathbf{f}(\mathbf{x}) + \epsilon(\mathcal{I} - \mathcal{P})[\mathbf{f}(\mathbf{y}) - \mathbf{f}(\mathbf{x})], \tag{E2}$$

$$\delta\dot{\mathbf{v}} = [(1 - \epsilon)\mathcal{I} + \epsilon\mathcal{P}]\mathbf{Df}\delta\mathbf{v}, \tag{E3}$$

where \mathcal{I} is the identity operator and \mathcal{P} is a projection operator onto a coarser grid system.

The coupling term in the slave system is designed so that the null space of \mathcal{P} , that is, the variation that cannot be resolved by the coarse-grained description, is attracted to the master system. The modified sensitivity is expected to be stabilized by being blurred by the operator \mathcal{P} . In particular, if $\epsilon = 1$, then the sensitivities can be traced by the coarser-resolution linear model $\delta\dot{\mathbf{v}} = \mathcal{P}\mathbf{Df}\delta\mathbf{v}$. To illustrate how the stabilization works, suppose we have a simple unstable system and a projection operator

$$\mathbf{Df} = \begin{bmatrix} \lambda_1 & 0 \\ 0 & \lambda_2 \end{bmatrix}, \quad \mathcal{P} = \frac{1}{2} \begin{bmatrix} 1 & 1 \\ 1 & 1 \end{bmatrix}, \tag{E4}$$

where $\lambda_1 > 0$, $\lambda_2 < 0$, and $\lambda_1 + \lambda_2 < 0$. Then, the growth of the \mathbf{v} -system is written, in

Gebbie et al. (2006), who applied this type of regularization to ocean data assimilation, successfully used a coarser resolution adjoint OGCM for an eddy-permitting state estimation.

REFERENCES

- Abarbanel, H. D. I., M. Kostuk, and W. Whartenby, 2010: Data assimilation with regularized nonlinear instabilities. *Quart. J. Roy. Meteor. Soc.*, **136 (648)**, 769–783.
- Barclay, A., P. E. Gill, and J. B. Rosen, 1998: SQP methods and their application to numerical optimal control. *International series of numerical mathematics*, 207–222.
- Benettin, G., L. Galgani, A. Giorgilli, and J. M. Strelcyn, 1980: Lyapunov characteristic exponents for smooth dynamical systems and for Hamiltonian systems; a method for computing all of them. Part 1: Theory. *Meccanica*, **15 (1)**, 9–20.
- Buizza, R., 1994: Sensitivity of optimal unstable structures. *Quart. J. Roy. Meteor. Soc.*, **120 (516)**, 429–451.
- Courtier, P., J. N. Thépaut, and A. Hollingsworth, 1994: A strategy for operational implementation of 4D-Var, using an incremental approach. *Quart. J. Roy. Meteor. Soc.*, **120 (519)**, 1367–1387.
- Cullen, M. J. P., 2010: A demonstration of 4D-Var using a time-distributed background term. *Quart. J. Roy. Meteor. Soc.*, **136 (650)**, 1301–1315.
- Duane, G. S., J. J. Tribbia, and J. B. Weiss, 2006: Synchronicity in predictive modelling: a new view of data assimilation. *Nonlinear Processes in Geophysics*, **13 (6)**, 601–612.

- Evensen, G., 1997: Advanced data assimilation for strongly nonlinear dynamics. *Mon. Wea. Rev.*, **125** (6), 1342–1354.
- Gebbie, G., P. Heimbach, and C. Wunsch, 2006: Strategies for nested and eddy-permitting state estimation. *J. Geophys. Res.*, **111** (C10), C10 073.
- Gratton, S., A. Lawless, and N. Nichols, 2008: Approximate Gauss-Newton methods for nonlinear least squares problems. *SIAM Journal on Optimization*, **18** (1), 106–132, doi: 10.1137/050624935.
- Hansen, J. A. and C. Penland, 2007: On stochastic parameter estimation using data assimilation. *Physica D: Nonlinear Phenomena*, **230** (1), 88–98.
- Hoteit, I., B. Cornuelle, A. Köhl, and D. Stammer, 2005: Treating strong adjoint sensitivities in tropical eddy-permitting variational data assimilation. *Quart. J. Roy. Meteor. Soc.*, **131** (613), 3659–3682.
- Hoteit, I. and A. Köhl, 2006: Efficiency of reduced-order, time-dependent adjoint data assimilation approaches. *Journal of Oceanography*, **62** (4), 539–550.
- Johnson, C., B. J. Hoskins, and N. K. Nichols, 2006: A singular vector perspective of 4D-Var: Filtering and interpolation. *Quart. J. Roy. Meteor. Soc.*, **131** (605), 1–19.
- Kapral, R., R. Livi, G. Oppo, and A. Politi, 1994: Dynamics of complex interfaces. *Physical Review E*, **49** (3), 2009.
- Kardar, M., G. Parisi, and Y. Zhang, 1986: Dynamic scaling of growing interfaces. *Physical Review Letters*, **56** (9), 889–892.

- Köhl, A. and D. Stammer, 2008: Decadal sea level changes in the 50-year gecco ocean synthesis. *J. Climate*, **21** (9), 1876–1890, doi:10.1175/2007JCLI2081.1.
- Köhl, A. and J. Willebrand, 2008: An adjoint method for the assimilation of statistical characteristics into eddy-resolving ocean models. *Tellus A*, **54** (4), 406–425.
- Lawless, A. S., S. Gratton, and N. K. Nichols, 2005: An investigation of incremental 4D-Var using non-tangent linear models. *Quart. J. Roy. Meteor. Soc.*, **131** (606), 459–476.
- Lea, D. J., T. W. N. Haine, M. R. Allen, and J. A. Hansen, 2002: Sensitivity analysis of the climate of a chaotic ocean circulation model. *Quart. J. Roy. Meteor. Soc.*, **128** (586), 2587–2605.
- Legras, B. and R. Vautard, 1996: A guide to Liapunov vectors. *Proceedings 1995 ECMWF Seminar on Predictability*, Vol. 1, 143–156.
- Luenberger, D. G., 1964: Observing the state of a linear system. *IEEE Transactions on Military Electronics*, **8** (2), 74–80.
- Masuda, S., et al., 2010: Simulated rapid warming of abyssal north pacific waters. *Science*, **329** (5989), 319–322.
- Mazloff, M. R., P. Heimbach, and C. Wunsch, 2010: An eddy-permitting Southern Ocean state estimate. *J. Phys. Oceanogr.*, **40** (5), 880–899.
- Noh, Y. and H. J. Kim, 1999: Simulations of temperature and turbulence structure of the oceanic boundary layer with the improved near-surface process. *J. Geophys. Res.*, **104**, 15.

- Pazó, D., I. G. Szendro, J. López, and M. A. Rodríguez, 2008: Structure of characteristic Lyapunov vectors in spatiotemporal chaos. *Physical Review E*, **78** (1), 016 209.
- Pecora, L. M. and T. L. Carroll, 1990: Synchronization in chaotic systems. *Physical Review Letters*, **64** (8), 821–824.
- Philander, S. G. H., W. J. Hurlin, and R. C. Pacanowski, 1986: Properties of long equatorial waves in models of the seasonal cycle in the tropical Atlantic and Pacific Oceans. *J. Geophys. Res.*, **91** (C12), 14 207–14 211.
- Primo, C., I. Szendro, M. Rodríguez, and J. Gutiérrez, 2007: Error growth patterns in systems with spatial chaos: from coupled map lattices to global weather models. *Physical Review Letters*, **98** (10), 108 501.
- Pyragas, K., 1993: Predictable chaos in slightly perturbed unpredictable chaotic systems. *Physics Letters A*, **181** (3), 203–210.
- So, P., E. Ott, and W. P. Dayawansa, 1994: Observing chaos: Deducing and tracking the state of a chaotic system from limited observation. *Physical Review E*, **49** (4), 2650–2660.
- Stammer, D., et al., 2002: Global ocean circulation during 1992–1997, estimated from ocean observations and a general circulation model. *J. Geophys. Res.*, **107**, 3118, doi:10.1029/2001JC000888.
- Sugiura, N., T. Awaji, S. Masuda, T. Mochizuki, T. Toyoda, T. Miyama, H. Igarashi, and Y. Ishikawa, 2008: Development of a four-dimensional variational coupled data assimilation system for enhanced analysis and prediction of seasonal to interannual climate variations. *J. Geophys. Res.*, **113** (C10), C10 017.

- Trémolet, Y., 2006: Accounting for an imperfect model in 4D-Var. *Quart. J. Roy. Meteor. Soc.*, **132** (621), 2483–2504.
- Trémolet, Y., 2007: Incremental 4D-Var convergence study. *Tellus A*, **59** (5), 706–718.
- Tsujino, H., M. Hirabara, H. Nakano, T. Yasuda, T. Motoi, and G. Yamanaka, 2011: Simulating present climate of the global ocean-ice system using the Meteorological Research Institute Community Ocean Model (MRI.COM): simulation characteristics and variability in the Pacific sector. *Journal of Oceanography*, **67**, 449–479.
- Tsujino, H., T. Motoi, I. Ishikawa, M. Hirabara, H. Nakano, G. Yamanaka, and T. Yasuda, 2010: Meteorological Research Institute Community Ocean Model Version 3 (MRI.COM3) Manual. Technical Report of Meteorological Research Institute 59, Meteorological Research Institute, Tsukuba, Japan. 241pp.
- Wunsch, C. and P. Heimbach, 2007: Practical global oceanic state estimation. *Physica D: Nonlinear Phenomena*, **230** (1), 197–208.
- Yang, S. C., et al., 2006: Data Assimilation as Synchronization of Truth and Model: Experiments with the Three-Variable Lorenz System. *J. Atmos. Sci.*, **63** (9), 2340–2354.
- Yaremchuk, M., D. Nechaev, and G. Panteleev, 2009: A Method of Successive Corrections of the Control Subspace in the Reduced-Order Variational Data Assimilation. *Mon. Wea. Rev.*, **137** (9), 2966–2978.
- Zhu, J. and M. Kamachi, 2000: The role of time step size in numerical stability of tangent linear models. *Mon. Wea. Rev.*, **128** (5), 1562–1572.

Zhu, J., M. Kamachi, and D. Wang, 2002: Estimation of air-sea heat flux from ocean measurements: An ill-posed problem. *J. Geophys. Res.*, **107** (C10), 3159, doi:10.1029/2001JC000995.

List of Figures

- 1 Schematic views of two chaotic systems that are close at the starting period. Two degrees of freedom for each system are shown as axes, one of which is linearly stable, whereas the other is unstable. Uncoupled systems diverge with time (left), whereas coupled systems synchronize (right) because of the attractive force between the two unstable variables. 44
- 2 The first approximate backward Lyapunov vector for case 1, the original model, indicated with $\log(|\delta\text{SST}|)$. The quantity is dimensionless because of normalization. The corresponding Lyapunov exponent is 1.51 day^{-1} . 45
- 3 The first approximate backward Lyapunov vector for case 2, with a prescribed vertical diffusion coefficient, indicated with $\log(|\delta T(z = 100 \text{ m})|)$. The quantity is dimensionless because of normalization. The corresponding Lyapunov exponent is -0.001 day^{-1} . 46
- 4 The first approximate backward Lyapunov vector for case 3, with a partially prescribed vertical diffusion coefficient, indicated with $\log(|\delta T(z = 100 \text{ m})|)$. The quantity is dimensionless because of normalization. The corresponding Lyapunov exponent is -0.001 day^{-1} . 47

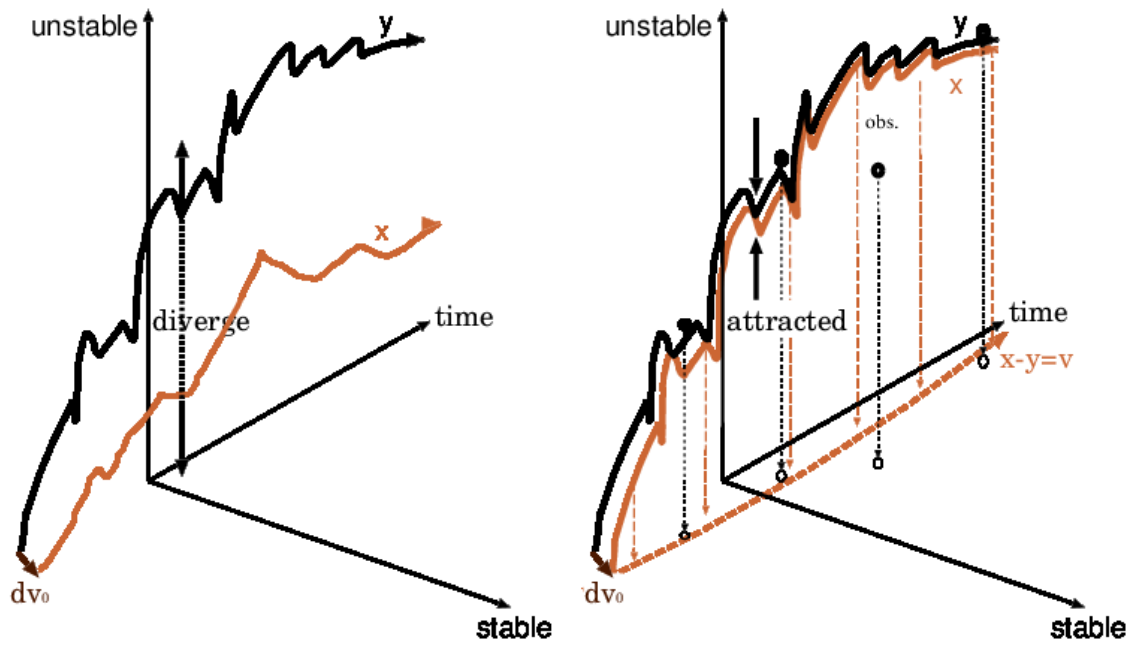


FIG. 1. Schematic views of two chaotic systems that are close at the starting period. Two degrees of freedom for each system are shown as axes, one of which is linearly stable, whereas the other is unstable. Uncoupled systems diverge with time (left), whereas coupled systems synchronize (right) because of the attractive force between the two unstable variables.

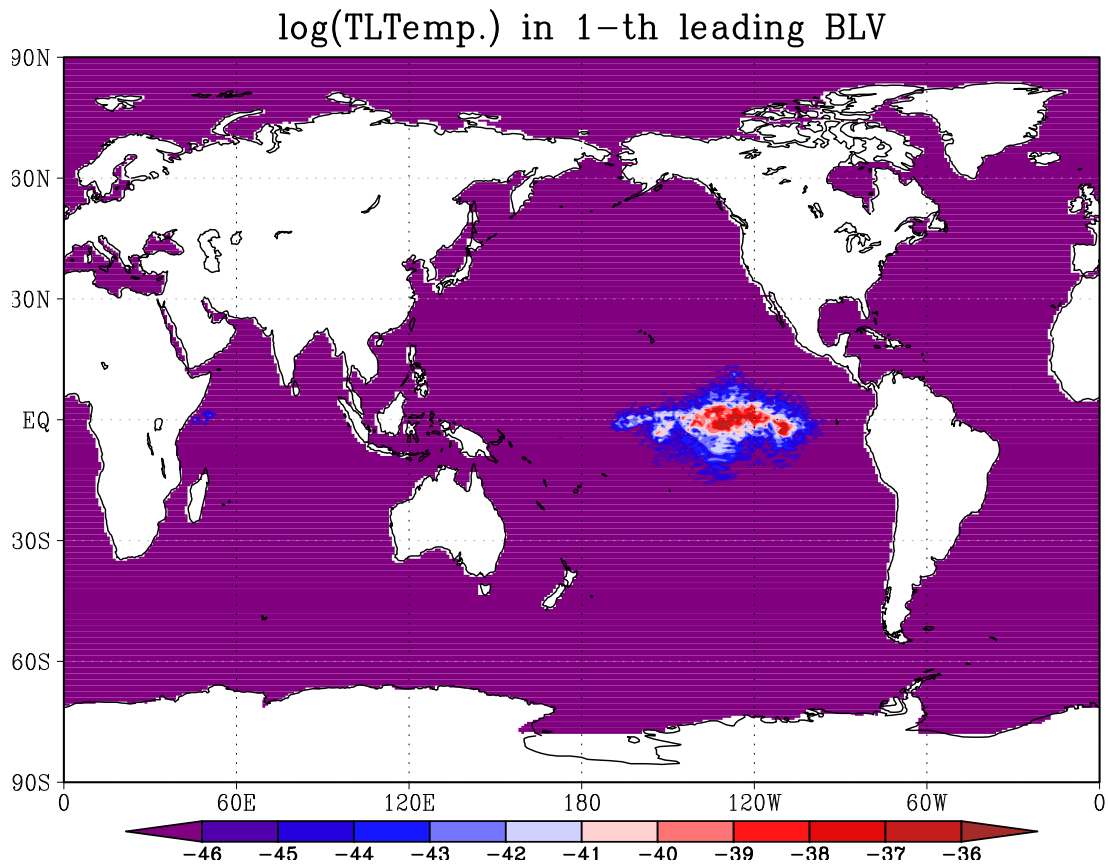


FIG. 2. The first approximate backward Lyapunov vector for case 1, the original model, indicated with $\log(|\delta\text{SST}|)$. The quantity is dimensionless because of normalization. The corresponding Lyapunov exponent is 1.51 day^{-1} .

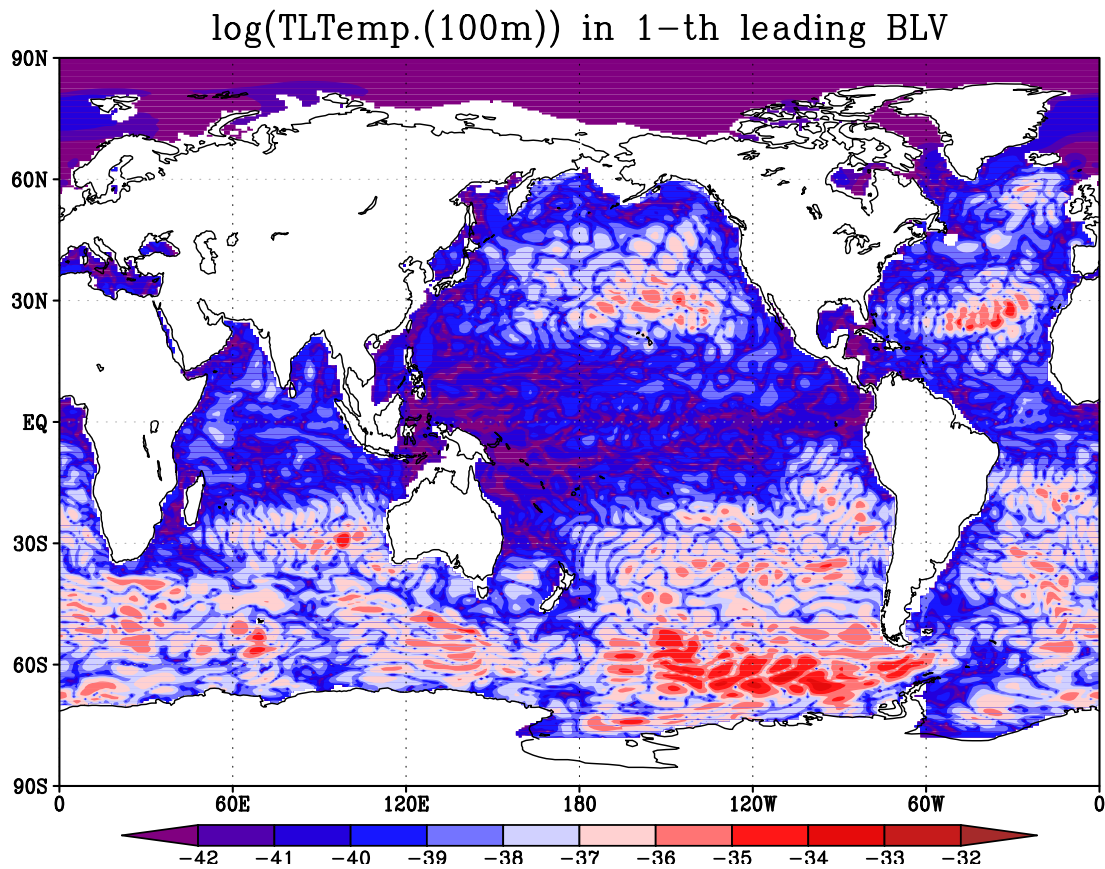


FIG. 3. The first approximate backward Lyapunov vector for case 2, with a prescribed vertical diffusion coefficient, indicated with $\log(|\delta T(z = 100 \text{ m})|)$. The quantity is dimensionless because of normalization. The corresponding Lyapunov exponent is -0.001 day^{-1} .

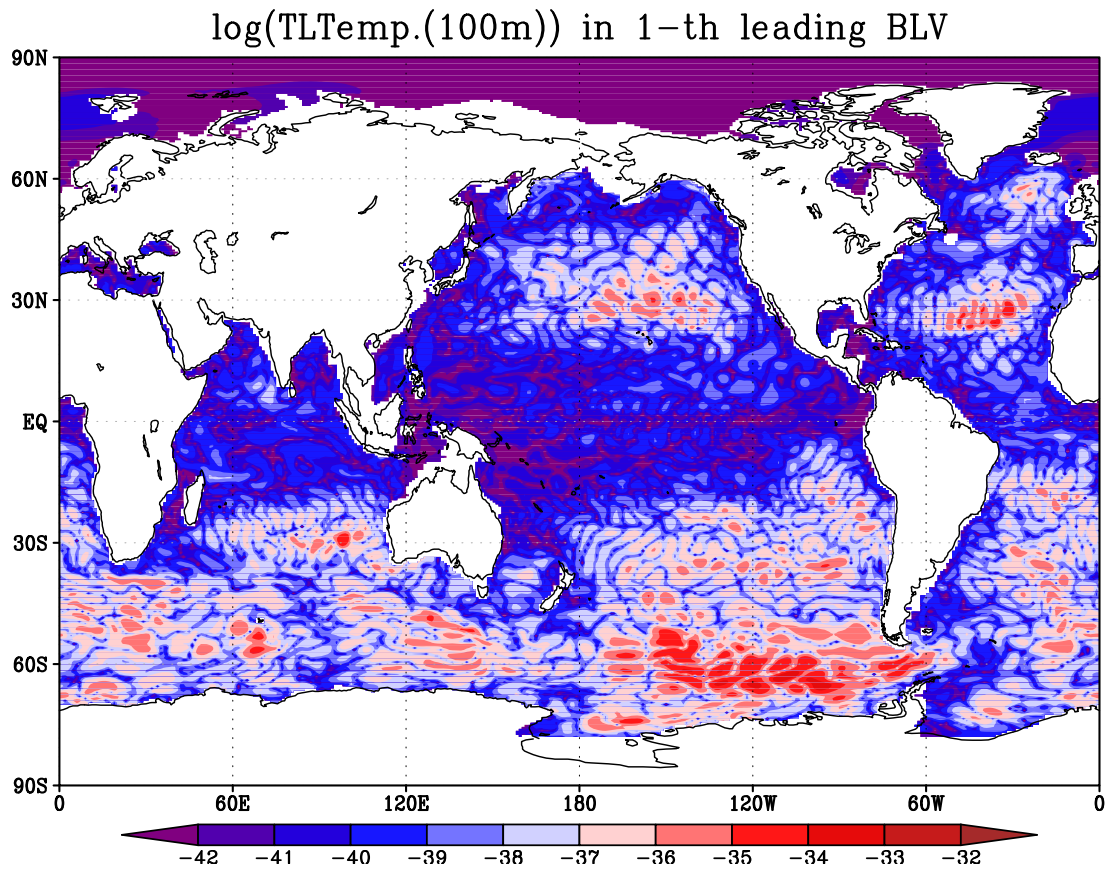


FIG. 4. The first approximate backward Lyapunov vector for case 3, with a partially prescribed vertical diffusion coefficient, indicated with $\log(|\delta T(z = 100 \text{ m})|)$. The quantity is dimensionless because of normalization. The corresponding Lyapunov exponent is -0.001 day^{-1} .